# Biochemical and Biophysical Characterization of OmpG: A Monomeric Porin[†]

Sean Conlan,[‡,§] Yong Zhang,[‡,§] Stephen Cheley,[‡] and Hagan Bayley*[,‡,||]

*Department of Medical Biochemistry & Genetics, The Texas A&M University System Health Science Center, College Station, Texas 77843-1114, and Department of Chemistry, Texas A&M University, College Station, Texas 77843-3255*

*Received May 10, 2000; Revised Manuscript Received July 26, 2000*

ABSTRACT: A recombinant form of the porin OmpG, OmpGm, lacking the signal sequence, has been expressed in *Escherichia coli*. After purification under denaturing conditions, the protein was refolded in the detergent Genapol X-080, where it gained a structure rich in $\beta$ sheet as evidenced by a CD spectrum similar to that of the native form. Electrophoretic analysis and limited proteolysis experiments suggested that refolded OmpGm exists in at least three forms. Nevertheless, the recombinant protein formed uniform channels in planar bilayers with a conductance of 0.81 nS (1 M NaCl, pH 7.5). Previous biochemical studies had suggested that OmpG is a monomeric porin, rather than the usual trimer. Bilayer recordings substantiated this proposal; voltage-induced closures occurred consistently in a single step, and channel block by $Gd^{3+}$ lacked the cooperativity seen with the trimeric porin OmpF. The availability of milligram amounts of a monomeric porin will be useful both for basic studies of porin function and for membrane protein engineering.

To produce channels and pores with new properties, our laboratory is applying protein engineering to membrane proteins (*1*−*4*). The bacterial porins (*5*−*8*) are favorable targets for these studies (*9, 10*). The porins determine the permeability of the outer membrane of Gram-negative bacteria. Major porins from *E. coli*, OmpF,[1] OmpC, and PhoE, allow the free diffusion of molecules smaller than ~600 Da. In addition to these nonspecific porins, there exist selective porins that are permeable to small molecules and ions, but allow only a limited assortment of large molecules to pass, for instance the maltodextrin-specific LamB.

Porins do not contain the lengthy continuous sequences of hydrophobic amino acids that constitute the membrane-spanning α-helices of many membrane proteins. Indeed, early studies using circular dichroism and infrared spectroscopy on the *E. coli* porin OmpF showed that it was composed primarily of $\beta$ sheet (*11*) and was perhaps a $\beta$ barrel (*12, 13*). Only about 10 residues are required to span the bilayer as a $\beta$ strand, in which only every other side chain is expected to be hydrophobic. Since the early work, many porins have been examined by crystallography; the atomic-resolution structures are strikingly similar despite the lack of amino acid sequence homology (*7, 14*). Porins are indeed $\beta$ barrels of 16 or 18 antiparallel strands, and the functional units consist of three $\beta$ barrels arranged about a central axis. Moreover, all outer membrane proteins examined to date (*8, 15*−*17*) are $\beta$ barrels, although some have been shown through structural studies to be monomers (*15, 17*), and in one case to be a dimer (*16*).

Porin trimers are generally resistant to SDS at room temperature (*11, 18*). For example, the trimers run as discrete bands upon SDS−polyacrylamide gel electrophoresis. Natural or overexpressed recombinant porins and other outer membrane proteins that have been denatured in urea, guanidinium salts, or SDS can be refolded, usually by dilution into detergent (*8, 19*−*21*). In the case of the porin from *Rhodopseudomonas blastica*, the crystal structure of the protein, refolded after extraction from inclusion bodies obtained from *E. coli*, showed that the exact native structure is regained (*22*).

Electrical recordings have been made with numerous porins, most often in planar bilayers or by patching giant liposomes. The major porins typically have a "restriction" loop that folds into the aqueous pore creating a constriction that contributes to size exclusion and selectivity. They form highly conductive channels, but the values of the unitary conductances are not strictly related to the dimensions of the pores, as seen in structural studies, or to their ability to transport macromolecules, for example, in liposome swelling assays (*5*−*8*). Nevertheless, most of the general diffusion (nonspecific) porins have a unitary conductance in the range of 0.5−1 nS per monomer subunit in 1 M salt. Voltage-dependent channel closures are usually seen at high trans-

[†] This work was supported by the DOE and the ONR. Sean Conlan was the recipient of an AASERT (ONR) award.

* Correspondence should be addressed to this author at the Department of Medical Biochemistry & Genetics, The Texas A&M University System Health Science Center, 440 Reynolds Medical Building, College Station, TX 77843-1114. Tel: (979) 845-7047, fax: (979) 862-2416, email: bayley@tamu.edu.

[‡] Department of Medical Biochemistry & Genetics, The Texas A&M University System Health Science Center.

[§] The first two authors contributed equally to this work

[||] Department of Chemistry, Texas A&M University.

[1] Abbreviations: CD, circular dichroism; DEAE, diethylaminoethyl; IPTG, isopropyl $\beta$-D-thiogalactoside; EDTA, ethylenediaminetetraacetic acid; Hepes, *N*-(2-hydroxyethyl)piperazine-*N*′-2-ethanesulfonic acid; LB medium, Luria Bertani medium; Omp, outer membrane protein; OmpF, outer membrane protein F, a porin; OmpFm, OmpF with the signal sequence replaced by a methionine codon; OmpG, outer membrane protein G, a porin; OmpGm, OmpG with the signal sequence replaced by a methionine codon; SDS, sodium dodecyl sulfate; SDS−PAGE, SDS−polyacrylamide gel electrophoresis; Tris, tris(hydroxymethyl)-aminomethane; PCR, polymerase chain reaction; PMSF, phenylmethylsulfonyl fluoride.

10.1021/bi001065h CCC: $19.00 
Published on Web 09/01/2000

membrane potentials (above ± 100 mV) (*23*), and often occur in three steps, reflecting the trimeric structure of the proteins [for review, see (*6, 24, 25*)].

The subject of the present study, OmpG, is a porin from *E. coli* K-12 that was found during a selection for mutants with increased membrane permeability. Specifically, expression of OmpG allows the growth of *E. coli* strains lacking LamB in the presence of maltodextrins as the sole carbon source (*26*). OmpG is unrelated in sequence to other outer membrane proteins. It is a 301 amino acid polypeptide, with the first 21 residues comprising a signal sequence (*27*). No crystal structure for OmpG exists, but a 16-stranded barrel has been predicted from the amino acid sequence (*27*). The channel lumen is ~20 Å in diameter, as estimated by liposome swelling (*27*). This large functional diameter may reflect the lack of a restriction loop. Another interesting characteristic of OmpG is that it appears to be monomeric in that it migrates as a monomer in SDS−polyacrylamide gels. However, there are other porins that are thought to be trimeric that do not resist SDS, for example, PIA from *Neisseria gonorrheae* (*28, 29*). Cross-linking experiments with dimethyl suberimidate and formaldehyde also indicated that OmpG is a monomer (*27*), but this approach can be criticized because OmpG possesses few lysine residues.

The $\beta$ barrel is an especially favorable structure with which to explore the introduction of new properties into transmembrane pores (*1*). In our laboratory, such studies have been performed on the heptameric pore-forming toxin α-hemolysin. To eliminate some of the complications inherent in dealing with a multisubunit structure, we have sought a single-chain transmembrane barrel. The initial characterization of OmpG (*27*) suggested that it would be an ideal candidate. We show here that OmpG can be overexpressed in a T7-based system, that the protein can be purified in denatured form and refolded, and that the refolded molecule has the biophysical properties expected of a monomeric porin.

## MATERIALS AND METHODS

*Chemicals*. Genapol X-080 detergent was from Fluka (Milwaukee, WI). Proteinase K was from GibcoBRL (Gaithersburg, MD). DEAE Sepharose was from Amersham Pharmacia Biotech (Piscataway, NJ). Unless otherwise noted, additional reagents were from Sigma (St. Louis, MO).

*Cloning and Strains*. The coding sequence for OmpG was amplified from *E. coli* XL-10 Gold (Stratagene, La Jolla, CA) genomic DNA using the following primers: forward, 5′-TAG GGC CAT ATG AAA AAG TTA TTA; reverse, 5′-CTA AAG CTT TTA TCA GAA CGA GTA. The amplified DNA was cloned into the Topo-TA plasmid (Invitrogen, Carlsbad, CA). The insert was then removed by digestion with *Nde*I and *Hin*dIII and ligated into a pT7 expression vector, pT7-SMC (*30*), which had been digested with the same enzymes. The insert from pT7-SMC was sequenced and matches the published coding sequence for OmpG (GenBank, gbbct:ecu49400). To express mature OmpG (designated OmpGm), a second insert was made, in which the region encoding the signal sequence was replaced with a methionine codon, by using the primer set: forward, 5′-TAG CAT ATG GAG GAA AGG AAC GAC; reverse, 5′-CTA AAG CTT TTA TCA GAA CGA GTA. The OmpF gene was amplified with the primers: forward, 5′-TAG CAT ATG ATG AAG CGC AAT; reverse, 5′-CTA AAG CTT CTA TTA GAA CTG GTA. The amplified DNA was cloned into the Topo-TA plasmid and then inserted into the prepared pT7 vector, as described above. The insert was sequenced and matches the sequence for OmpF (GenBank, gbbct: ECOOMPF). A mature version of OmpF (OmpFm) was made by replacing the region encoding the signal sequence with a methionine codon by using the primer set: forward, 5′-TAG CAT ATG GCA GAA ATC TAT AAC AAA GAT GG; reverse, 5′-CTA AAG CTT CTA TTA GAA CTG GTA. Cloning was carried out in XL-10 Gold cells. Protein expression was carried out in porin-deficient PC2889 cells [BL21(DE3)ΔlamB ompR] from the Netherlands Culture Collection (Utrecht, Netherlands). The cells were transformed with the pLysE plasmid for tight control of expression from the T7 promoter (*31*) and grown in the presence of chloramphenicol (20 $\mu$g/mL) to maintain the plasmid. These cells are designated PC2889E.

*Secondary Structure Prediction*. The sequence of OmpGm was analyzed with the program om_topo_predict (http://strucbio.biologie.uni-konstanz.de/~kay/om_topo_predict.html), which predicts the topology of porins (*32*). Further analysis was performed by using the neural net program BTPRED (http://www.biochem.ucl.ac.uk/bsm/btpred/index.html) (*33*) to predict $\beta$ turns. The Kyte−Doolittle hydropathy profile of OmpGm was generated using the GREASE program (*34*) (http://biology.ncsa.uiuc.edu/).

*Expression and Purification*. The porins OmpGm and OmpFm were expressed and purified by the same procedure. For example, to obtain OmpGm, a starter culture of transformed PC2889E cells was grown at 37 °C in LB medium (5 mL) containing chloramphenicol (20 $\mu$g/mL) and ampicillin (50 $\mu$g/mL). The culture was used to inoculate LB medium (400 mL) containing ampicillin (50 $\mu$g/mL). After the $OD_{600}$ reached a value of 0.7, expression of OmpGm was induced with 0.5 mM IPTG. The cells were grown for a further 2 h at 37 °C, and then recovered by centrifugation and frozen. The cell pellet was cracked with lysis buffer (5 mL: 200 $\mu$g/mL hen egg white lysozyme, 1 mM PMSF, 10 mM Tris·HCl, 1 mM EDTA, pH 8.0) on ice for 15 min. The lysate was pelleted at 60000*g* in a TL100.2 rotor with a Beckman TL-100 ultracentrifuge. The resulting insoluble fraction was washed once in 1 M urea, 1% Triton X-100, in 10 mM Tris·HCl, pH 8.0 (10 mL), and once in 1 M urea in 10 mM Tris·HCl, pH 8.0 (10 mL). The pellet was then dissolved at 4 °C in fresh denaturation buffer (50 mL: 8 M urea, 10 mM Tris·HCl, pH 8.0). The dissolved pellet was filtered through a 0.22 $\mu$m filter (Corning, polyethersulfone) and loaded onto a DEAE-Sepharose column (12.5 mL bed) equilibrated with denaturation buffer. The bound protein was then eluted with a linear gradient of NaCl (150 mL, 0−500 mM) in denaturation buffer. The fractions containing the protein were pooled (~20 mL) and dialyzed against 2 L of folding buffer [1% (w/v) Genapol X-080 in 10 mM Tris·HCl, pH 8.0] with one buffer change at 4 °C. The protein concentration was determined by measuring the absorbance at 280 nm in 8 M urea using an extinction coefficient of 84 950 $M^{-1}$ $cm^{-1}$ for OmpGm (*35*). This procedure typically yielded ~5 mg of purified OmpGm.

Gel-purified protein was prepared by electrophoresis of material taken prior to DEAE Sepharose chromatography

(see above) in a 12.5% SDS−polyacrylamide gel, with 0.1 mM thioglycolate in the running buffer to scavenge free radicals. The gel was stained with 0.1% Coomassie Blue in water for 1 h. After destaining with water, the desired band was excised. The gel slice was frozen at −20 °C overnight, and crushed with a disposable pestle. The crushed gel was incubated overnight at 4 °C in 10 mM sodium phosphate buffer, pH 7.0, containing 2% Genapol X-080 (500 $\mu$L for 100 mg of gel). The slurry was filtered with a 0.2 $\mu$m cellulose acetate spin filter (Rainin, Emeryville, CA). The recovery of protein in the filtrate was 30−50% as estimated by analytical SDS−PAGE and densitometry.

*Circular Dichroism*. CD measurements were carried out with an Aviv 62DS circular dichroism spectrometer (Lakewood, NJ) with a 10 mm path length cuvette. The protein (0.025 mg/mL, 0.75 $\mu$M) was in 10 mM Tris·HCl, pH 8.0, 0.1% Genapol X-080. Each sample was scanned 5 times from 300 to 200 nm with a 0.5 nm step size. To produce the plot in Figure 3, the data were corrected for background and converted to mean residue ellipticity using the equation:

$$[\Theta] = (100 \times \Theta_{obs})/([prot]_{mM} \times l_{cm} \times n)$$

where $n$ is the number of amino acid residues and $l$ is the path length in centimeters.

Secondary structure composition was analyzed by using the CONTIN program (http://www2.umdnj.edu/cdrwjweb/) (*36*). The RAW2CON program was first used to normalize the data, using the concentration of 0.025 mg/mL. The data were analyzed by using all three reference sets provided with CONTIN as indicated in Table 1.

*Gel Filtration*. Gel filtration chromatography was performed on an ÄKTA Purifier liquid chromatography system equipped with a Superdex 200 HR 10/30 column (Amersham Pharmacia Biotech, Piscataway, NJ). The column was equilibrated with 3 column volumes of folding buffer supplemented with 150 mM NaCl, and the sample (100 $\mu$L) was applied and eluted with the equilibration buffer. The absorption of the eluate was followed at 220 and 280 nm. For some experiments, the concentration of detergent was 0.05% (w/v), which produced only minimal differences in the elution profiles.

*Proteolysis*. Limited proteolysis was performed for the indicated times at room temperature in a final volume of 5 $\mu$L containing OmpGm (400 $\mu$g/mL) and proteinase K (5 $\mu$g/mL) in 10 mM Tris·HCl, pH 8.0, 0.2% Genapol X-080. The reaction was stopped by the addition of 10 mM PMSF, followed by a 5 min incubation at room temperature. Samples were then mixed with loading buffer and analyzed in a 12.5% SDS−polyacrylamide gel.

*Planar Lipid Bilayer Recordings.* Planar lipid bilayer membranes were formed by applying 1,2-diphytanoyl-*sn*-glycero-3-phosphocholine (Avanti Polar Lipids, Birmingham, AL), dissolved in highly purified pentane (Burdick & Jackson, Allied Signal Inc., Muskegon, MI), to a 120−150 $\mu$m diameter orifice in a 25 $\mu$m thick Teflon film (Goodfellow, Malvern, PA) separating the cis and trans compartments of the apparatus (*37*). The orifice was pretreated with hexadecane/pentane (1:10 v/v) (hexadecane from Aldrich, Milwaukee, WI) before bilayer formation.

Unless specified, the compartments contained 1 M NaCl, 5 mM Hepes·NaOH, pH 7.5. For ion-selectivity measurements, various concentrations of NaCl or KCl with 5 mM Hepes (Hepes·NaOH for NaCl solutions, Hepes·KOH for KCl solutions), pH 7.5, were used. OmpGm or OmpFm that had been diluted into a final concentration of 0.5% Genapol X-080 in 10 mM sodium phosphate, pH 7.0, was added to the cis compartment to a final concentration of 0.5−5 ng/mL. Voltage was applied across the bilayer with Ag/AgCl electrodes in 1.5% agarose (Bio-Rad, Hercules, CA) containing 3 M KCl. The cis compartment was grounded, and a positive potential indicates a higher potential in the trans chamber. A positive current is one in which cations flow from the trans to the cis side. The current was amplified with an Axopatch 200B amplifier (Axon Instruments, Foster City, CA) and filtered with a Bessel filter (model 900, Frequency Devices, Haverhill, MA). The signal was then acquired by a personal computer after digitization with a DigiData 1200A A/D board (Axon Instruments) and analyzed with Clampex 7.0 or FETCHAN software (Axon Instruments).

*I*−*V* relationships were determined for the primary conducting states of single OmpGm channels by recording current values immediately after the transient capacitative currents arising from the voltage steps.

The relative permeabilities toward $Na^+$, $K^+$, and $Cl^-$ were determined by the analysis of reversal potentials according to the Goldman−Hodgkin−Katz (GHK) equation, by using the appropriate activity coefficients (*38*). The potential offset was adjusted to zero before formation of the bilayer.

## RESULTS

*Cloning*. The coding sequence for OmpGm was amplified by PCR, sequenced, and found to match exactly the sequence published in GenBank. A BLAST search (http://www.ncbi.nlm.nih.gov) of the *E. coli* K-12 genome (*39*) was performed to confirm that OmpG is not strain-specific. The genome contained a sequence with a 100% match at the nucleotide level.

*Secondary Structure and Topology Predictions.* Analysis of the amino acid sequence of OmpGm with conventional programs for secondary structure prediction (e.g., GOR, PELE, CHOFAS) produces results that are implausible when the CD spectrum, which is characteristic of predominant $\beta$ sheet, is considered (*27*). The prediction of a 16-stranded $\beta$ barrel (*27*) is in rough agreement with the size calculated for the pore by liposome swelling (*27*). However, two of the predicted transmembrane strands (numbers 10 and 13) do not possess a well-defined alternating pattern of hydrophobic and hydrophilic residues, and removal of these two strands, and the adjustment of two others (numbers 7 and 11), generates a more plausible structure (Figure 1C). The lower end of the transmembrane barrel (as shown in Figure 1C) carries an obvious aromatic belt. Strikingly, five of the strands in this region display two aromatic side chains.

The theoretical pore diameter of Fajardo and colleagues was calculated by using a strand-to-strand distance of 4.5 Å, giving a diameter of about 23 Å, which is in agreement with the liposome swelling data. This calculation, however, assumes that the $\beta$ strands are oriented normal to the plane of the membrane. It is more likely that the strands are tilted relative to the membrane plane (*40, 41*), giving a larger strand-to-strand distance in the plane of the membrane. To

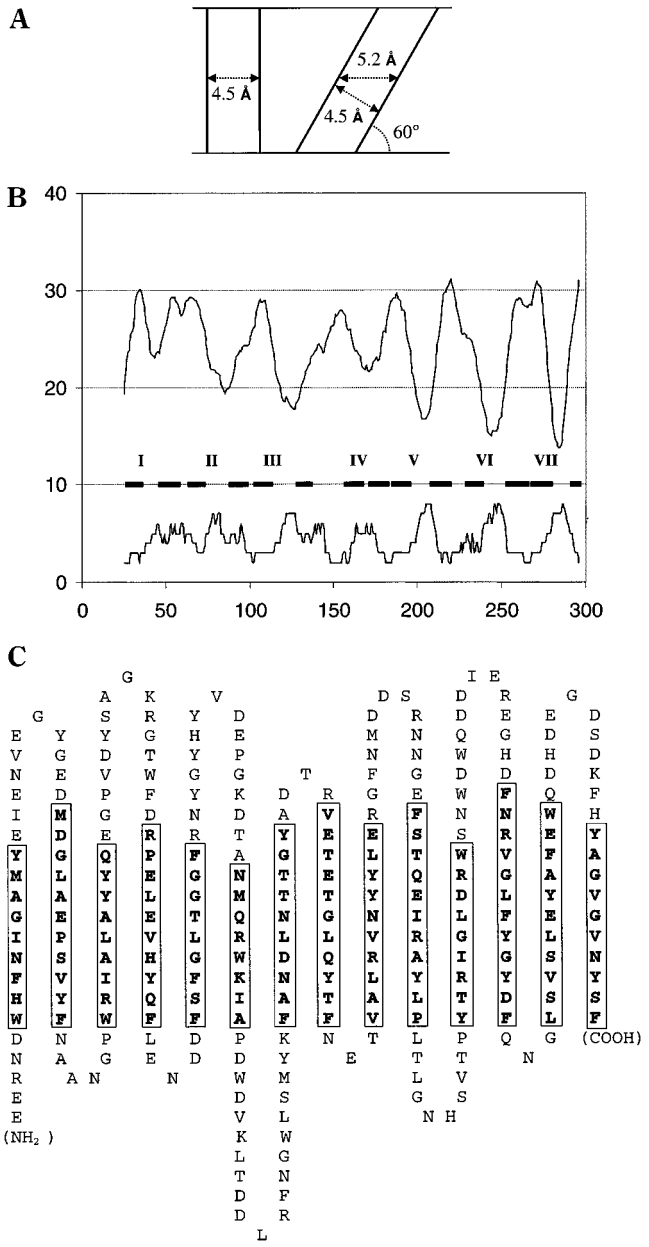


FIGURE 1: Revised topology of OmpGm. (A) The tilt of a $\beta$ barrel affects the diameter of the channel. (B) Computer analysis of topology. Both programs used the amino acid sequence of OmpGm as input. The upper trace was generated from GREASE, by smoothing the plot with 10-point adjacent averaging with Microcal Origin 5.0 (Microcal Software Inc., Northampton, MA). GREASE plots relative side-chain hydrophobicity; a seven amino acid window was used. The lower trace was generated by om_topo_predict. The *X* axis represents amino acid number; the numbering scheme is based on full-length OmpG. The *Y* axis displays the units for both programs. In the case of the GREASE plot, lower values are more hydrophilic and higher values are more hydrophobic. While OmpGm is hydrophilic overall, there are seven obvious minima in the plot. The program om_topo_predict produces a number from 1 to 8, where 1−3 indicate periplasmic residues and 6−8 indicate extracellular residues. Between the two traces are roman numerals which highlight the seven extracellular loops and bars which represent the predicted $\beta$ strands. (C) The predicted 14-strand topology for OmpGm.

form the same diameter barrel (23 Å), a 14-stranded barrel would be tilted 61° (Figure 1A).

The sequence of OmpGm was analyzed with additional programs to predict secondary structure and topology with respect to the bilayer. A hydropathy plot for the protein was generated using GREASE (*34*) and shows seven obvious regions of low hydropathy corresponding to the predicted extracellular loops (Figure 1B). The program om_topo_predict (*32*) is a neural net (with no programmed sense of hydropathy) designed to predict porin topology. It also predicted the location of the extracellular loops successfully, with the exception of the most N-terminal residues (Figure 1B). Finally, the neural net program BTPRED (*33*) was used to predict $\beta$ turns, in this case with less success. Collectively, the computer predictions strongly support the 14-stranded model (Figure 1C).

*Expression and Purification.* A great deal of work on porins has been carried out with renatured protein (*8*), and we decided to follow this approach. Since full-length OmpG contains a signal sequence, a mature version called OmpGm was made genetically, by replacing the signal sequence codons with a methionine codon. OmpGm was successfully overexpressed, purified, and refolded, by a straightforward procedure based on a modification of the protocol used for pea root plastid porin (*42*). Briefly, the insoluble fraction from an expression culture was denatured with 8 M urea. OmpGm was then purified under denaturing conditions by using DEAE Sepharose ion exchange chromatography and refolded by dialysis into a 1% solution of the nonionic detergent Genapol X-080.

A number of outer membrane proteins possess different mobilities upon SDS−polyacrylamide gel electrophoresis depending on whether the sample is heated before analysis (*43*). Native OmpG migrates as a 28 kDa band before heating in SDS and a 34 kDa band afterward. However, this heat modifiability is lost upon dialysis, although the protein remains active (*27*). When the purified and refolded protein obtained here was analyzed by SDS−polyacrylamide gel electrophoresis, it was found to migrate as at least three forms. A fraction of the protein ran as a 34 kDa species, below which a diffuse 33 kDa band and a sharp 29 kDa band were seen (Figure 2B). When the sample was heated at 100 °C, only the 34 kDa species was seen (Figure 2B).

Limited proteolysis of preparations of OmpGm suggested that the 33 and 29 kDa bands are not just artifacts of electrophoresis, but exist in solution. The uppermost, 34 kDa, species was highly sensitive to protease, while the 33 and 29 kDa bands were degraded more slowly under the same conditions (Figure 2B). At low concentrations of protease, a 29 kDa product was observed after proteinase K treatment (Figure 2B). The 29 kDa fragment is present regardless of heating, indicating that it is indeed a fragment and not the heat-modifiable band.

*Circular Dichroism.* The circular dichroism spectrum of OmpGm is similar to the published spectrum of native OmpG (*27*), which indicates that the protein is correctly folded at least in terms of its secondary structure, despite the distribution between the various electrophoretic bands (Figure 3 and Table 1). The spectrum was analyzed with the CONTIN program to estimate the amount of $\beta$ sheet, $\alpha$ helix, and turn (*36*). The three reference sets provided with the software were used, and each produced different results (Table 1). This is not surprising, considering that it is difficult to accurately quantify secondary structure in proteins that contain predominantly $\beta$ structure (*44*). Nevertheless, although the numbers vary considerably, it is obvious from the data that the protein is composed primarily of $\beta$ sheet.

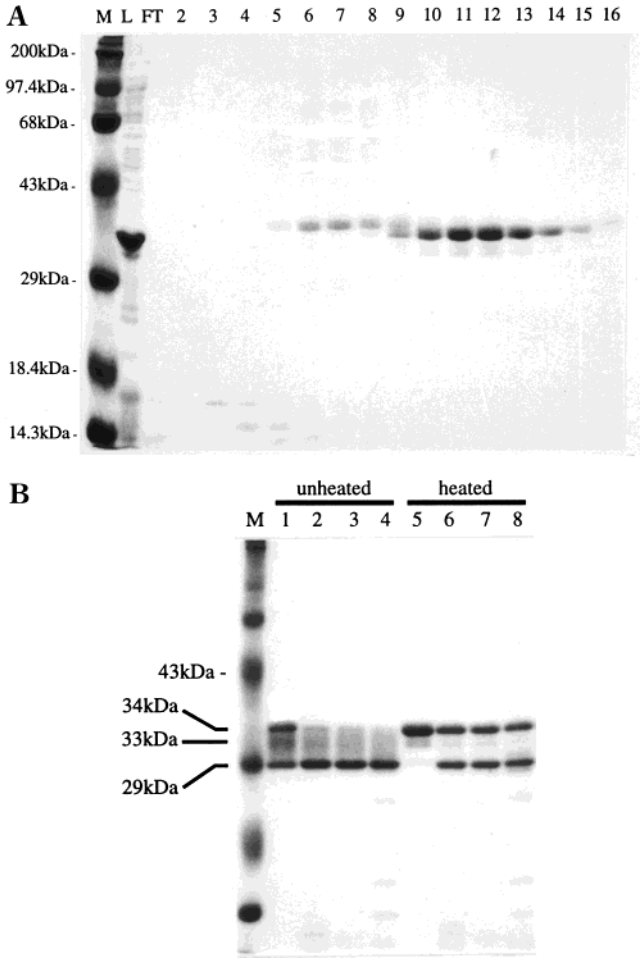


FIGURE 2: Analysis of OmpGm by SDS−polyacrylamide gel electrophoresis. 12.5% gels were used and stained with Coomassie Blue. (A) Purification of OmpGm on a DEAE Sepharose column eluted with a gradient of NaCl. Fraction numbers are shown above the gel lanes. M, molecular weight markers; L, protein as loaded in 8 M urea; FT, flow-through fraction. OmpGm began to elute at around fraction 9, which contains ~200 mM NaCl. The samples were heated in sample buffer before electrophoresis. (B) Refolded OmpGm in 1% Genapol X-080 exists in multiple forms. Lanes 1−4 are a proteolysis time course. Lane 1: untreated OmpGm; lanes 2−4: OmpGm treated with proteinase K (5 $\mu$g/mL) for 5, 20, and 60 min, respectively. The samples were treated with PMSF, mixed with SDS-containing sample buffer, and loaded onto the gel without heating. Lanes 5−8: same as lanes 1−4 except that the samples were heated at 100 °C for 5 min before loading. Note that the unproteolyzed protein exists in three forms with apparent masses of 34, 33, and 29 kDa (lane 1). The protein used in this experiment had been stored at 4 °C for 3 months.

*Gel Filtration.* Analytical gel filtration was performed on refolded OmpGm to verify that it was monomeric in detergent solution, as suggested by SDS−PAGE. Surprisingly, OmpGm elutes rapidly from a Superdex 200 HR column in 1% Genapol X-080, appearing close to the ferritin marker (440 kDa, Stokes' radius 61 Å). The column profile was similar regardless of the distribution of the protein between the various electrophoretic bands. Furthermore, OmpFm refolded under the same conditions, which was monomeric, as expected (*20*) when analyzed by SDS−polyacrylamide gel electrophoresis, elutes at the same position as OmpGm. Similar results were used in concluding that recombinant *Neisseria gonorrheae* porin exists as a trimer in solution (*29*). However, our data suggest that no definitive judgment can be made by this approach. It is not surprising that porins behave nonideally upon gel filtration since their Stokes' radii are likely to be larger than those of globular proteins of the same mass; they contain large water-filled interiors and presumably bind a wide belt of detergent.

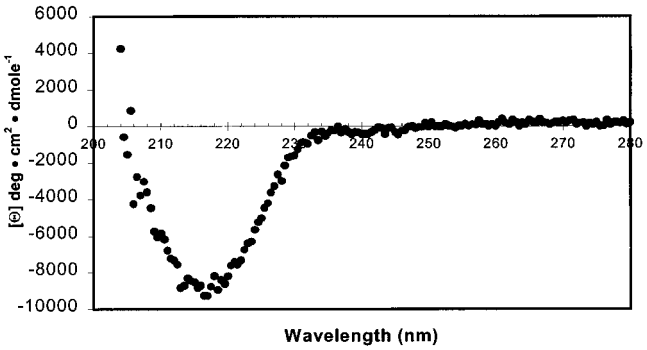


FIGURE 3: CD spectrum of OmpGm. OmpGm in 1% Genapol X-080, 10 mM Tris·HCl, pH 8.0, was diluted 10-fold with 10 mM Tris·HCl, pH 8.0, to a final concentration of 0.025 mg/mL (0.75 $\mu$M). The sample was scanned in a 10 mm path length cuvette, as described under Materials and Methods. Analysis of the protein by SDS−PAGE, followed by quantification using Scion Image (Scion Corp., Frederick, MD), showed the sample to be composed of the following species: 34 kDa band, 51%; 33 kDa (broad band), 29%; 29 kDa band, 20%.

Table 1: Summary of Secondary Structure Calculations for OmpGm Based on CD Data Analyzed with CONTIN

| alpha | beta | turn | remainder | reference set |
|---|---|---|---|---|
| 0.18 ± 0.02 | 0.55 ± 0.02 | 0.04 ± 0.02 | 0.23 ± 0.02 | *a* |
| 0.15 ± 0.04 | 0.71 ± 0.05 | 0.08 ± 0.04 | 0.07 ± 0.07 | *b* |
| 0.16 ± 0.01 | 0.46 ± 0.01 | 0.19 ± 0.01 | 0.18 ± 0.01 | *c* |

[a] The original 16 proteins (*36*). [b] The original 16 proteins, plus 4 denatured proteins (*62*). [c] The original 16 proteins, plus poly-L-glutamate (*63*).

*OmpGm Forms Ion-Conducting Channels in Planar Lipid Bilayers.* Stepwise increases in membrane conductance were observed when OmpGm was added to the cis side of a planar bilayer. Of 92 observed events, 84% were around 0.8 nS in magnitude (Figures 4and 5). Only 3% of the events were 3 times this value and probably represent unresolved multiple insertions. Therefore, the primary conductance state was taken to be ~0.8 nS. After single insertion events at −40 mV, the OmpGm channels remained largely open, although transient closures of variable amplitude were observed (Figure 4). Measurement of 16 $I-V$ curves for single OmpGm channels yielded a minimal unitary conductance of 0.81 ± 0.02 nS. OmpGm channels exhibit linear $I-V$ relationships at membrane voltages from −100 to +100 mV (Figure 6). By contrast, 89% of the insertion events for OmpFm were ~2.6 nS (Figure 5B). Based on 18 $I-V$ curves for single channels, OmpFm has a minimal unitary conductance of 2.76 ± 0.05 nS, roughly 3 times larger than OmpGm.

OmpGm is weakly cation-selective. With 1 M NaCl cis and 300 mM NaCl trans, the reversal potential of OmpGm is 19.4 ± 0.9 mV ($n = 4$) (Figure 7). With 1 M KCl cis and 325 mM KCl trans, the reversal potential of OmpGm is 17.3 ± 0.1 mV ($n = 2$) (Figure 7). When interpreted according to the GHK equation, these measurements yield the permeability ratios: $P_{Cl}:P_{Na}:P_K = 0.17:1:1$. At higher salt gradients, OmpGm shows lower anion/cation permeability ratios, e.g., $P_{Cl}:P_{Na}:P_K = 0.12:0.92:1$, with 1 M NaCl or KCl cis and

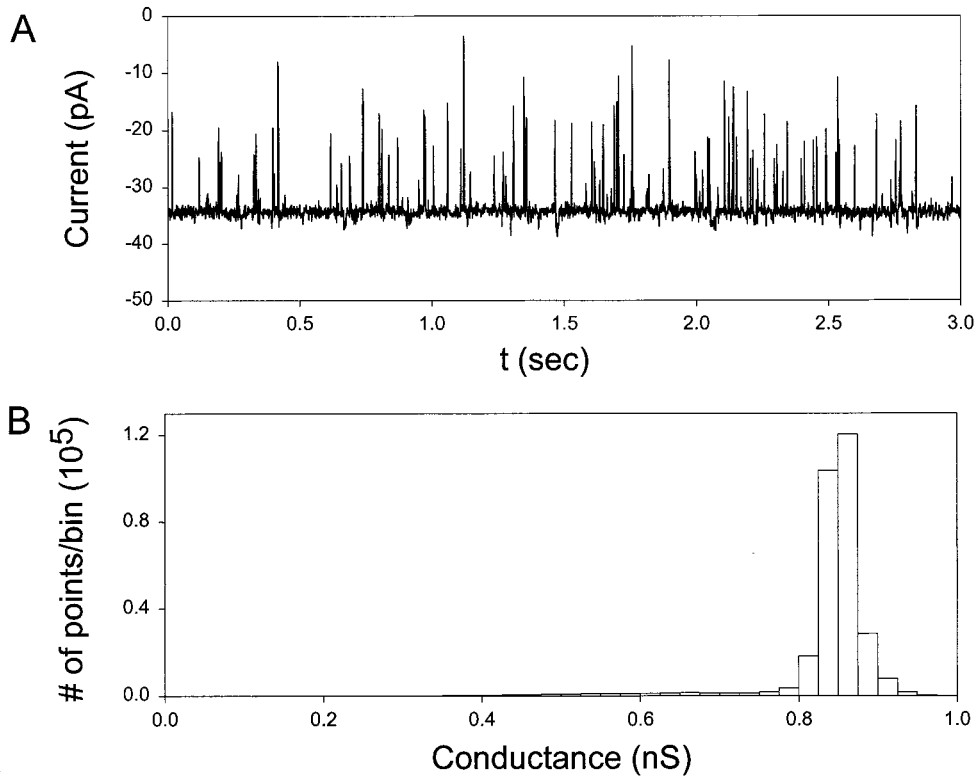


FIGURE 4: Single channel recording of OmpGm in a planar bilayer. (A) Current recording of a single OmpGm channel. (B) Histogram of the amplitude distribution of the recording in (A). The cis and trans chambers both contained 1 M NaCl, 5 mM Hepes·NaOH, pH 7.5. The transmembrane potential was −40 mV.

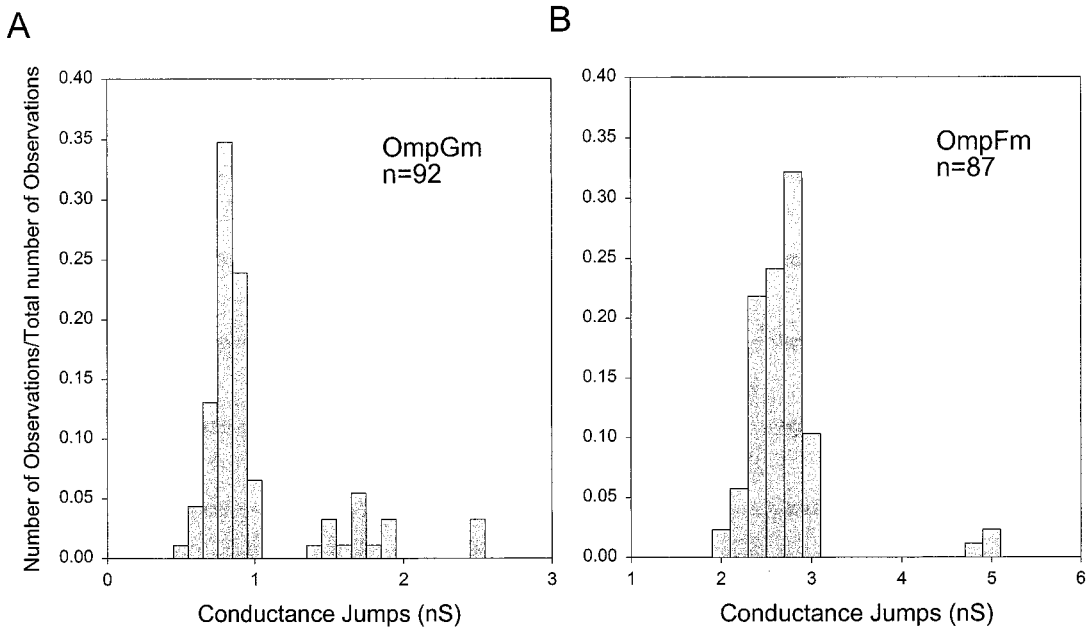


FIGURE 5: Histograms showing the magnitudes of insertion events for (A) OmpGm and (B) OmpFm. The conditions were the same as in Figure 4.

100 mM NaCl or KCl trans. Under similar conditions, 1 M NaCl or KCl cis and 300 mM NaCl trans or 325 mM KCl trans, the permeability ratios of OmpFm were determined to be $P_{Cl}$:$P_{Na}$:$P_K$ = 0.24:1.25:1, consistent with previously published data (*45*−*47*).

*OmpGm Has a Symmetrical Current*−*Voltage Dependence and Closes in a Single Step.* Unlike OmpF and PhoE, which have asymmetrical current−voltage relationships (*48*), OmpGm was gated by both positive and negative membrane potentials (Figure 8). In addition, in 33 of 34 voltage-induced closures of single OmpGm channels, only a single closing step was observed (Figure 9B). The nonconforming event was a noisy two-step closure. In contrast, the "single" OmpFm channels showed three-step voltage-dependent closing (Figure 9A), which has also been documented in the literature (*49*−*52*).

*OmpGm Is Blocked by Gadolinium Ions.* $Gd^{3+}$ (1 mM trans) blocked OmpGm channels (Figure 10). The block

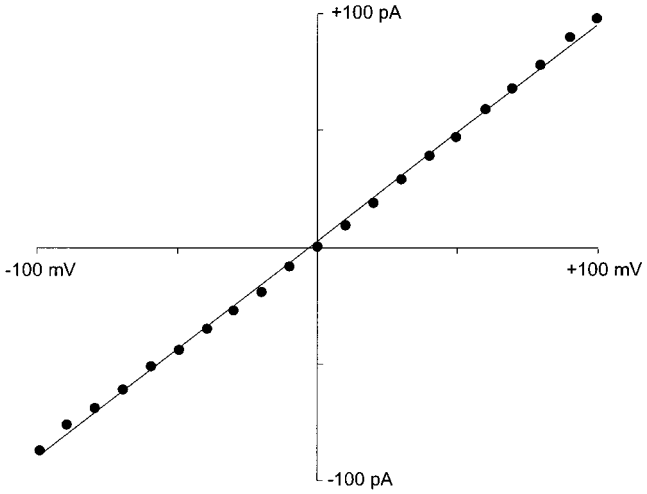


FIGURE 6: Representative $I-V$ relationship for a single OmpGm channel. The conditions were the same as in Figure 4.

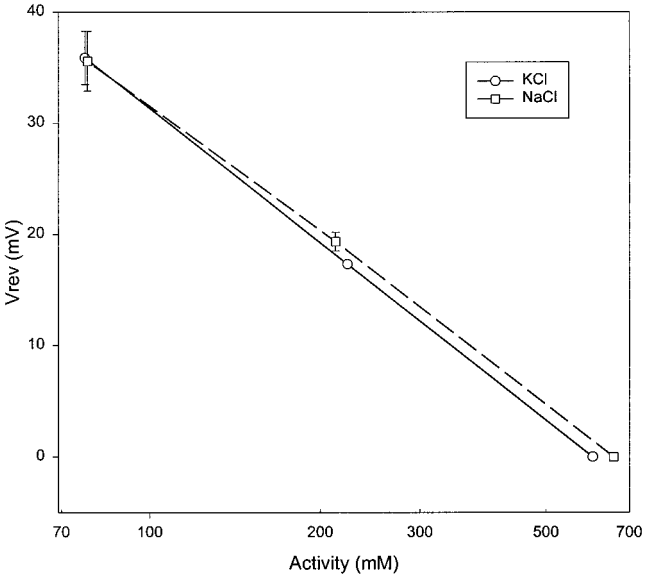


FIGURE 7: Reversal potential shifts of OmpGm in different salt gradients. (□) The cis chamber was filled with 1 M NaCl, and the trans chamber was filled with 1 M NaCl, 300 mM NaCl, or 100 mM NaCl. (○) The cis chamber was filled with 1 M KCl and the trans chamber with 1 M KCl, 325 mM KCl, or 100 mM KCl. The solutions also contained 5 mM Hepes, adjusted to pH 7.5. The salt concentrations are converted to activities in the figure. The slopes of the lines reveal reversal potentials for a 10-fold activity gradient: NaCl, 38 mV; KCl, 40 mV.

recovered partially after ~20 s at negative potentials, but not at positive potentials. $Gd^{3+}$ blocked OmpGm more potently at trans positive membrane potentials (Figure 11B, $IC_{50} = 408 \pm 72$ $\mu$M, $n = 9$, at −40 mV; $IC_{50} = 18.8 \pm 6.7$ $\mu$M, $n = 3$, at +40 mV, at steady state). OmpFm is also blocked by $Gd^{3+}$, which again showed voltage-dependent potency (Figure 11A, $IC_{50} = 1410 \pm 60$ $\mu$M, $n = 3$, at −40 mV; $IC_{50} = 108 \pm 37$ $\mu$M, $n = 3$, at +40 mV). Dose−inhibition curves for OmpGm and OmpFm show different slopes (Figure 11) with Hill coefficients at −40 mV of 1.39 ± 0.18 and 5.35 ± 0.67 for OmpGm and OmpFm, respectively ($n = 3$). Hill coefficients at +40 mV are 1.37 ± 0.16 and 3.51 ± 0.26 for OmpGm and OmpFm, respectively ($n = 3$).

## DISCUSSION

The biochemical and biophysical data presented in this paper extend our knowledge of the recently sequenced porin OmpG. We show that OmpG can be overexpressed, purified in denatured form, and refolded to yield functional protein. Importantly, strong evidence for the monomeric nature of OmpG was obtained through the analysis of single channel recordings, which revealed single-step closures and a lack of cooperativity in the blockade by $Gd^{3+}$ ions.

We propose a structural model for OmpG that differs significantly from that proposed previously (*27*). Two of the $\beta$ strands (strand 10: DDSRNNGEF, and strand 13: EIDDWQDW) in the original 16-stranded model are poor candidates as membrane-spanning segments, because of their high and nonalternating polarity. Elimination of these strands as membrane-spanning segments and adjustment of two additional strands (7 and 11) yield a barrel structure that is more appealing (Figure 1C). We also made a computer analysis of the OmpG sequence. Increasingly often, programs are being produced to predict structures for a class of proteins instead of all proteins. Proteins can be placed in the correct class based on limited structural and functional information: for example, in the case of OmpG, its CD spectrum and channel-forming ability. Analysis with recently developed algorithms produced a consensus in favor of the 14-stranded model for OmpG (Figure 1B,C).

We have shown that OmpG can be expressed at useful levels in inclusion bodies (~10 mg/L of culture). Like many other porins (*8*), OmpG can be folded by denaturation (in 8 M urea) followed by renaturation in detergent. The formation of a structure with a preponderance of $\beta$ sheet was confirmed by quantitative circular dichroism spectroscopy. The refolded OmpG exists in three interconvertible forms, distinguishable by SDS−polyacrylamide gel electrophoresis as 34, 33, and 29 kDa species. The 29 kDa form probably corresponds to a previously identified form of OmpG that displays a gel shift after heating (*27*). The gel shift of "6 kDa" is similar to that described for other heat-modifiable outer membrane proteins (*43*). We suggest that the 29 kDa species is the fully folded form of OmpG and that the 33 kDa form represents folding intermediates or off-pathway species. The three forms of OmpG appear to be in equilibrium as we have so far been unable to achieve complete conversion to the 29 kDa form. Further, the 29 kDa form extracted from *E. coli* membranes is converted to the 34 kDa species upon dialysis (*27*). If the 29 kDa species is the fully folded form of OmpG, the channels observed when our samples are applied to planar bilayers (see below) most likely originate by direct insertion of this form of the protein. Alternatively, channels might be formed if the 33 or 34 kDa species can complete folding upon incorporation into the bilayer.

Further information about OmpG, including evidence that the functional pore is a monomer, was obtained by single channel recording. Single channels of OmpG have a conductance of 0.81 nS at ±40 mV and exhibit characteristic voltage-dependent closures at transmembrane potentials above ±100 mV. Unlike OmpF (*49*−*52*), and many other porins (*24*, *28*, *53*−*56*), the voltage-dependent closures of OmpG occur in a single step. This indicates that OmpG is a monomer or that if OmpG is multimeric the closures are so tightly coupled as to be unresolvable on the microsecond

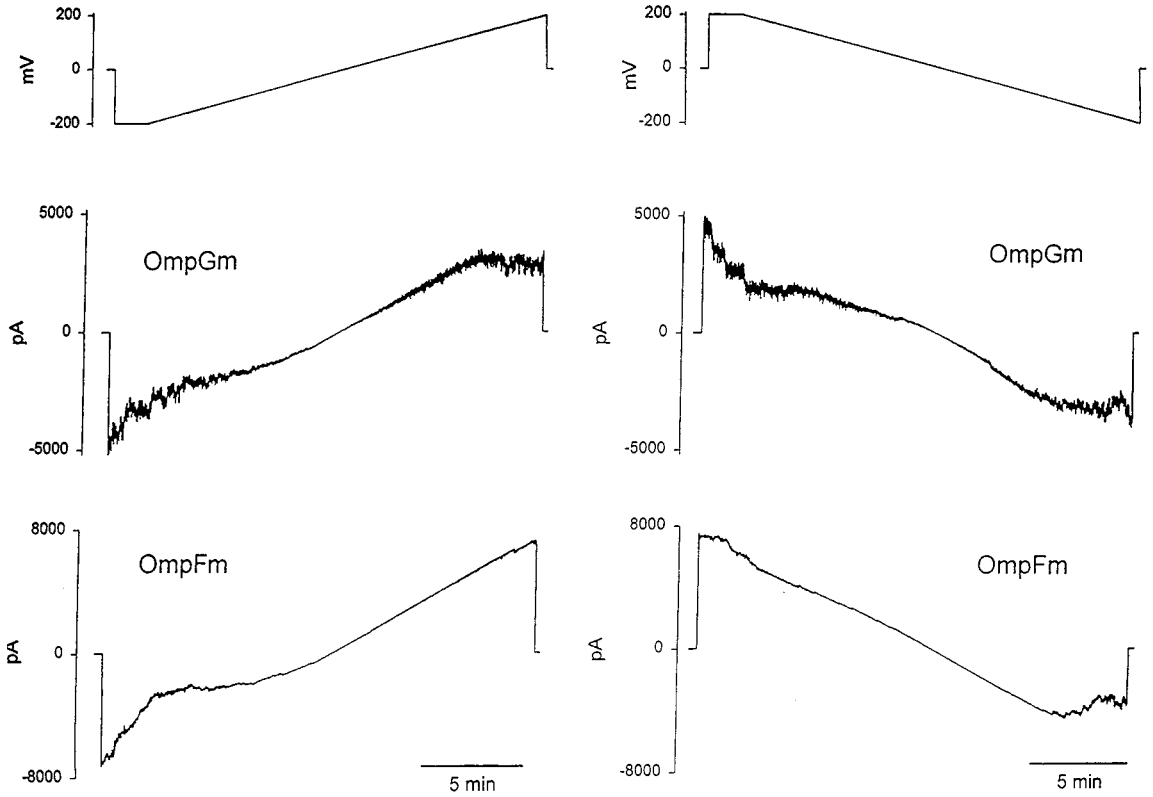


FIGURE 8: Voltage-dependent gating of OmpGm and OmpFm measured with voltage ramps. The upper panels are the voltage protocols. The middle and lower panels show the currents of OmpGm and OmpFm, respectively, in response to upward and downward ramps. The conditions were the same as in Figure 4.

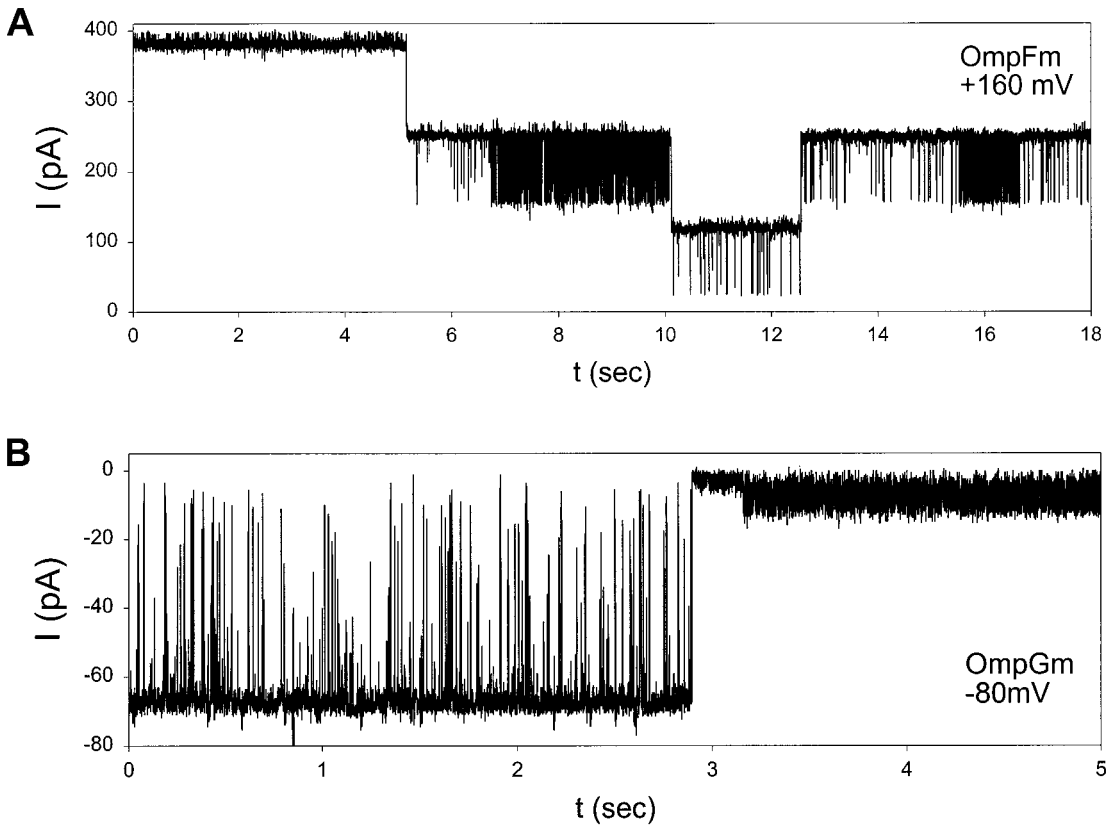


FIGURE 9: Current recordings showing voltage-dependent gating of OmpFm and OmpGm. (A) A three-step closure of OmpFm in response to a voltage step from +40 to +160 mV. (B) A single step closure of an OmpGm channel in response to a voltage step from 0 to −80 mV. The voltage steps were made before the starts of the traces. The conditions were the same as in Figure 4.

time scale. In addition, the blockade of OmpG by the trivalent cation $Gd^{3+}$ supports the existence of a monomer. While $Gd^{3+}$ interacts with OmpG with a Hill coefficient of 1.37−1.39, the Hill coefficient for OmpF is 3.51−5.35, indicating

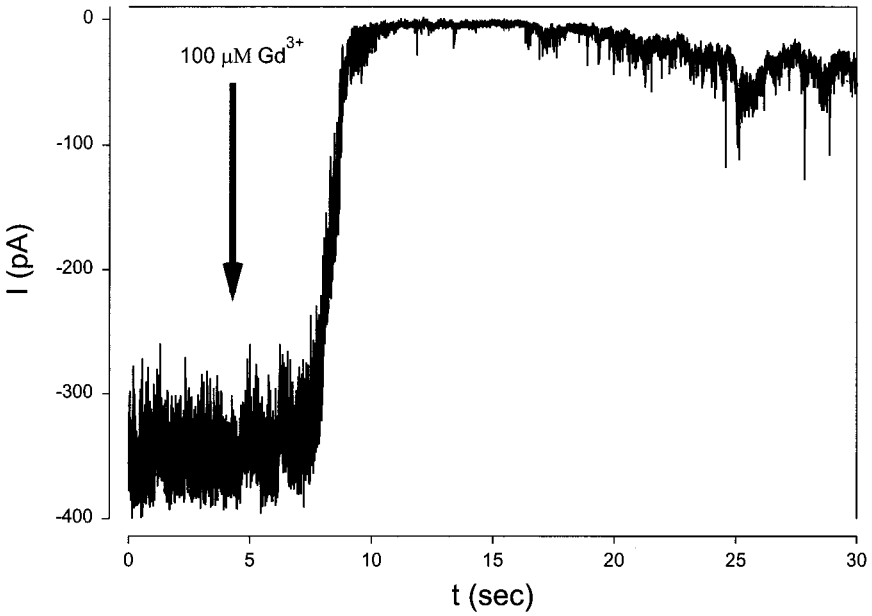


FIGURE 10: Current through OmpGm channels is blocked by $Gd^{3+}$. The arrow indicates the application of 1 mM $Gd^{3+}$ to the trans chamber. The membrane potential was held at −40 mV. At negative potentials, OmpGm channel activity recovers partially, usually after more than 10 s. The membrane contained 10−12 channels. The conditions were the same as in Figure 4.

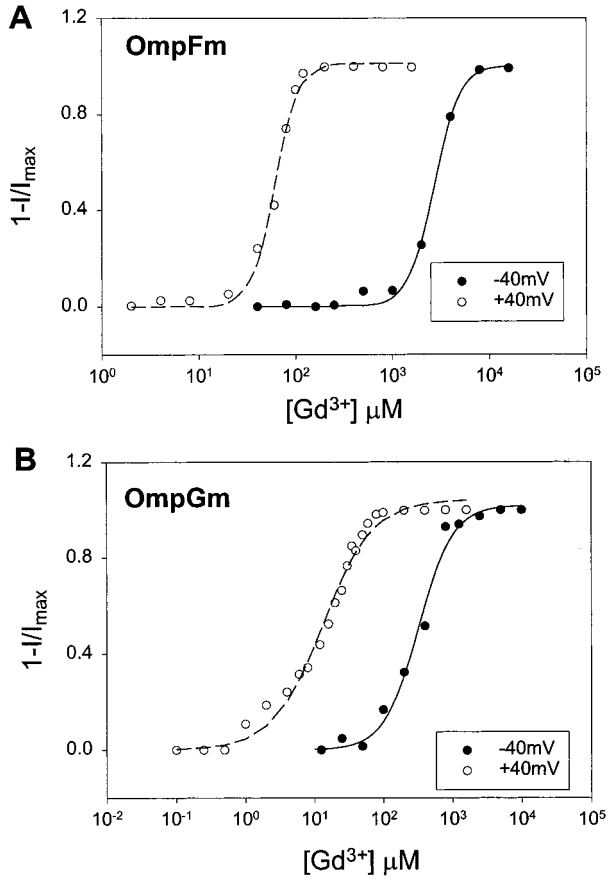


FIGURE 11: Steady-state $Gd^{3+}$ block of OmpGm and OmpFm at positive and negative transmembrane potentials. (A) Dose−inhibition curves of OmpFm at −40 mV (●) and +40 mV (○). (B) Dose−inhibition curves for OmpGm at −40 mV (●) and +40 mV (○). Both chambers contained 1 M NaCl, 5 mM Hepes·NaOH, pH 7.5. $Gd^{3+}$ was added to the trans chamber.

strong interaction between multiple binding sites. Although it is a less reliable measure than the gating kinetics or cooperativity of $Gd^{3+}$ block, the relatively low conductance of OmpG is also in keeping with a functional monomer. For example, most of the general diffusion (nonspecific) porins have a unitary conductance in the range of 0.5−1 nS per monomer subunit in 1 M salt (*5*−*8*). At 0.81 nS, the conductance of OmpG is in this range.

Trimerization of the major porins requires a hydrophobic interface between the subunits and a subunit−subunit interaction mediated by a latch formed by the loop L2 (*57*, *58*). However, there are no consensus sequences for the trimer interface, so it is impossible to tell whether OmpG would be expected to trimerize on this basis. Further, while most trimeric porins dissociate and unfold in a single transition, certain native (*29*) or mutant porins (*57*) can be dissociated into folded monomers, but it is not known whether these molecules are functional pores.

Despite the fact that it produces uniform single channels in bilayers, we should be cautious in concluding that refolded OmpG has exactly the same structure as the native protein. In the case of the porin from *Rhodopseudomonas blastica*, the crystal structure of the refolded protein was closely similar to that of the native protein (*22*). By contrast, native and refolded OmpA exhibit subtly different electrical properties (*59*). Once folded into a near-native form, there may be a high kinetic barrier to structural adjustments in $\beta$ barrels, due to the interstrand hydrogen bonds. Such a barrier would not exist in α helical membrane proteins.

The availability of milligram amounts of a monomeric porin will be useful both for basic studies of porin function and for membrane protein engineering. Previous studies of the electrical properties of porins have been conducted with trimers adding complexity to the interpretation of the results. Membrane protein engineering in our laboratory has focused on the heptameric pore formed by staphylococcal α-hemolysin (*1*, *60*). While heteroheptameric pores containing mutations or modifications at single sites can be made (*4*, *61*), the availability of a single-chain barrel will be a welcome addition to the field of protein design.

## ACKNOWLEDGMENT

We thank Dr. Hiroshi Nikaido for a preprint of the paper describing OmpG (*27*).

## REFERENCES

1. Bayley, H. (1999) *Curr. Opin. Biotechnol. 10*, 94−103.
2. Cheley, S., Braha, O., Lu, X., Conlan, S., and Bayley, H. (1999) *Protein Sci. 8*, 1257−1267.
3. Gu, L.-Q., Braha, O., Conlan, S., Cheley, S., and Bayley, H. (1999) *Nature 398*, 686−690.
4. Howorka, S., Movileanu, L., Lu, X., Magnon, M., Cheley, S., Braha, O., and Bayley, H. (2000) *J. Am. Chem. Soc. 122*, 2411−2416.
5. Jap, B. K., and Walian, P. J. (1996) *Physiol. Rev. 76*, 1073−1088.
6. Delcour, A. H. (1997) *FEMS Microbiol. Lett. 151*, 115−123.
7. Schirmer, T. (1998) *J. Struct. Biol. 121*, 101−109.
8. Buchanan, S. K. (1999) *Curr. Opin. Struct. Biol. 9*, 455−461.
9. Schulz, G. E. (1996) *Curr. Opin. Struct. Biol. 6*, 485−490.
10. Schmid, B., Maveyraud, L., Kromer, M., and Schulz, G. E. (1998) *Protein Sci. 7*, 1603−1611.
11. Rosenbusch, J. P. (1974) *J. Biol. Chem. 249*, 8019−8029.
12. Paul, C., and Rosenbusch, J. P. (1985) *EMBO J. 4*, 1593−1597.
13. Vogel, H., and Jähnig, F. (1986) *J. Mol. Biol. 190*, 191−199.
14. Pauptit, R. A., Schirmer, T., Jansonius, J. N., Rosenbusch, J. P., Parker, M. W., Tucker, A. D., Tsernoglou, D., Weiss, M. S., and Schulz, G. E. (1991) *J. Struct. Biol. 107*, 136−145.
15. Pautsch, A., and Schulz, G. E. (1998) *Nat. Struct. Biol. 5*, 1013−1017.
16. Snijder, H. J., Ubarretxena-Belandia, I., Blaaw, M., Kalk, K. H., Verheij, H. M., Egmond, M. R., Dekker, N., and Dijkstra, B. W. (1999) *Nature 401*, 717−721.
17. Vogt, J., and Schulz, G. E. (1999) *Structure 7*, 1301−1309.
18. Schindler, M., and Rosenbusch, J. P. (1984) *FEBS Lett. 173*, 85−89.
19. Surrey, T., and Jähnig, F. (1992) *Proc. Natl. Acad. Sci. U.S.A. 89*, 7457−7461.
20. Surrey, T., Schmid, A., and Jähnig, F. (1996) *Biochemistry 35*, 2283−2288.
21. Kleinschmidt, J. H., Wiener, M. C., and Tamm, L. K. (1999) *Protein Sci. 8*, 2065−2071.
22. Schmid, B., Krömer, M., and Schulz, G. E. (1996) *FEBS Lett. 381*, 111−114.
23. Bainbridge, G., Gokce, I., and Lakey, J. H. (1998) *FEBS Lett. 431*, 305−308.
24. Dargent, B., Hofmann, W., Pattus, F., and Rosenbusch, J. P. (1986) *EMBO J. 5*, 773−778.
25. Buehler, L. K., Kusumoto, S., Zhang, H., and Rosenbusch, J. P. (1991) *J. Biol. Chem. 266*, 24446−24450.
26. Misra, R., and Benson, S. A. (1989) *J. Bacteriol. 171*, 4105−4111.
27. Fajardo, D. A., Cheung, J., Ito, C., Sugawara, E., Nikaido, H., and Misra, R. (1998) *J. Bacteriol. 180*, 4452−4459.
28. Mauro, A., Blake, M., and Labarca, P. (1988) *Proc. Natl. Acad. Sci. U.S.A. 85*, 1071−1075.
29. Matsuka, Y. V., Dilts, D. A., Hoiseth, S., and Arumugham, R. (1998) *J. Protein Chem. 17*, 719−728.
30. Cheley, S., Malghani, M. S., Song, L., Hobaugh, M., Gouaux, J. E., Yang, J., and Bayley, H. (1997) *Protein Eng. 10*, 1433−1443.
31. Studier, F. W., Rosenberg, A. H., Dunn, J. J., and Dubendorff, J. W. (1990) *Methods Enzymol. 185*, 60−89.
32. Diederichs, K., Freigang, J., Umhau, S., Zeth, K., and Breed, J. (1998) *Protein Sci. 7*, 2413−2420.
33. Shepherd, A. J., Gorse, D., and Thornton, J. M. (1999) *Protein Sci. 8*, 1045−1055.
34. Kyte, J., and Doolittle, R. F. (1982) *J. Mol. Biol. 157*, 105−132.
35. Pace, C. N., Vajdos, F., Fee, L., Grimsley, G., and Gray, T. (1995) *Protein Sci. 4*, 2411−2423.
36. Provencher, S. W., and Glöckner, J. (1981) *Biochemistry 20*, 33−37.
37. Montal, M., and Mueller, P. (1972) *Proc. Natl. Acad. Sci. U.S.A. 69*, 3561−3566.
38. Hille, B. (1992) *Neuron 9*, 187−195.
39. Blattner, F. R., Plunkett, G., Bloch, C. A., Perna, N. T., Burland, V., Riley, M., Collado-Vides, J., Glasner, J. D., Rode, C. K., Mayhew, G. F., Gregor, J., Davis, N. W., Kilpatrick, H. A., Goeden, M. A., Rose, D. J., Mau, B., and Shao, Y. (1997) *Science 277*, 1453−1462.
40. Murzin, A. G., Lesk, A. M., and Chothia, C. (1994) *J. Mol. Biol. 236*, 1369−1381.
41. Murzin, A. G., Lesk, A. M., and Chothia, C. (1994) *J. Mol. Biol. 236*, 1382−1400.
42. Popp, B., Gebauer, S., Fischer, K., Flügge, I., and Benz, R. (1997) *Biochemistry 36*, 2844−2852.
43. Beher, M. G., Schnaitman, C. A., and Pugsley, A. P. (1980) *J. Bacteriol. 143*, 906−913.
44. Manavalan, P., and Johnson, W. C. (1987) *Anal. Biochem. 167*, 76−85.
45. Lakey, J. H., Watts, J. P., and Lea, E. J. A. (1985) *Biochim. Biophys. Acta 817*, 208−216.
46. Benz, R., Schmid, A., and Hancock, R. E. W. (1985) *J. Bacteriol. 162*, 722−727.
47. Hancock, R. E. W., Schmidt, A., Bauer, K., and Benz, R. (1986) *Biochim. Biophys. Acta 860*, 263−267.
48. Samartzidou, H., and Delcour, A. H. (1998) *EMBO J. 17*, 93−100.
49. Engel, A., Massalski, A., Schindler, H., Dorset, D. L., and Rosenbusch, J. P. (1985) *Nature 317*, 643−645.
50. Berrier, C., Coulombe, A., Houssin, C., and Ghazi, A. (1992) *FEBS Lett. 306*, 251−256.
51. Phale, P. S., Schirmer, T., Prilipov, A., Lou, K.-L., Hardmeyer, A., and Rosenbusch, J. P. (1997) *Proc. Natl. Acad. Sci. U.S.A. 94*, 6741−6745.
52. Bainbridge, G., Mobasheri, H., Armstrong, G. A., Lea, E. J. A., and Lakey, J. H. (1998) *J. Mol. Biol. 275*, 171−176.
53. Wiese, A., Schröder, G., Brandenburg, K., Hirsch, A., Welte, W., and Seydel, U. (1994) *Biochim. Biophys. Acta 1190*, 231−242.
54. Bishop, N. D., and Lea, E. J. A. (1994) *FEBS Lett. 349*, 69−74.
55. Andersen, C., Krones, D., Ulmke, C., Schmid, K., and Benz, R. (1998) *Eur. J. Biochem. 254*, 679−684.
56. Song, J., Minetti, C. A. S. A., Blake, M. S., and Colombini, M. (1998) *Biochim. Biophys. Acta 1370*,
57. van Gelder, P., and Tommassen, J. (1996) *J. Bacteriol. 178*, 5320−5322.
58. Phale, P. S., Philippsen, A., Kiefhaber, T., Koebnik, R., Phale, V. P., Schirmer, T., and Rosenbusch, J. P. (1998) *Biochemistry 37*, 15663−15670.
59. Arora, A., Rinehart, D., Szabo, G., and Tamm, L. K. (2000) *J. Biol. Chem. 275*, 1594−1600.
60. Bayley, H., Braha, O., and Gu, L.-Q. (2000) *Adv. Mater. 12*, 139−142.
61. Braha, O., Walker, B., Cheley, S., Kasianowicz, J. J., Song, L., Gouaux, J. E., and Bayley, H. (1997) *Chem. Biol. 4*, 497−505.
62. Venyaminov, S. Yu., Baikalov, I. A., Shen, Z. M., Wu, C.-S. C., and Yang, J. T. (1993) *Anal. Biochem. 214*, 17−24.
63. Sreerama, N., and Woody, R. W. (1993) *Anal. Biochem. 209*, 32−44.

BI001065H